# Simulating Structural Resistance of D&I Food Cans to Open Up Downgauging Potential

B. Liebscher[1], F. Knieps[1], I. Weinand[1]

[1]thyssenkrupp Rasselstein GmbH, Koblenzer Straße 141, Andernach, Germany

To reduce cost and increase the efficiency of D&I food cans, a lighter can with the same axial stability and paneling resistance is required. Axial stability depends on wall thickness, bead geometry (mainly bead depth) and tensile strength in the wall, whereas paneling resistance is a function of wall thickness, Young's modulus and bead geometry (mainly bead depth), with the bead depth having an opposite influence on paneling resistance and axial stability. FEA is used to find a bead geometry that satisfies both the paneling resistance and axial stability requirements. For a stable calculation of the paneling resistance, perturbation in the form of an eigenmode is required. The calculation time is significantly reduced by using an implicit solver with arc length method. When simulating axial stability, accurate modeling of the beginning of the flow curve is required. A weight reduction of 5% can be achieved by using next-generation high-strength D&I steel grades (e.g. rasselstein® D&I Solid).

## 1 Introduction

In the packaging steel market, demand for $CO_2$ and cost reduction goes along with downgauging ambitions to receive lighter cans. At the same time, there is a trend away from three-piece cans, which consist of a welded body, seamed bottom and lid, towards two-piece cans (also named D&I food can). D&I food cans are manufactured by draw and redraw of a cup and a subsequent ironing. This process has the advantage to avoid a welded body, which is more vulnerable regarding leakages. At the same time, a two- piece can line shows a higher profitability when operating at maximum capacity. Both, three- and two- piece cans must meet certain stability standards. In particular, a can must withstand a certain axial load and at the same time a certain paneling pressure to ensure a stable sterilization or pasteurization process. When aiming for a thickness reduction of the sheet metal, it must be ensured, that the defined stability requirements are kept. Thus, there is a trend towards higher strength materials. Materials as "rasselstein® D&I solid" offer a higher yield strength and a stronger hardening behavior, which results in a higher axial load resistance. However, the paneling pressure is not a function of the material strength but rather dependent on the can stiffness. This means, that sheet thickness, geometry (bead depth) and Young's modulus influence the resulting paneling pressure. Therefore, thickness reduction by using new generations of higher strength D&I steels always require the adaption of the can geometry. A higher bead depth leads to decreasing axial load while the paneling pressure increases. At this point, finite element analysis is of interest, to reduce cost intensive trial and error experiments. The general benefit of FE-simulation in the packaging steel industry was described by Köhl et al. fundamentally [1]. Both, simulation of axial load resistance and paneling pressure have not been investigated for D&I food cans so far. In a publication from Predictive Engineering Inc., the geometric nonlinear behavior of cylinders [2] was already shown. In addition, the need to pertub the geometry by using eigenvalue buckling mode shade was also demonstrated. Whang et al. simulated already axial load and paneling resistance for beaded cans and showed the optimization potential. They also noticed the need to consider eigenvalues for the simulation of paneling resistance [3]. In addition, a good overview on simulating structural resistance of metal container was given. However, only three-piece cans were considered in their investigation. Especially, to enable the use of FE-simulations in case of axial load resistance for D&I food cans the precise description of the yield strength in the can wall is crucial. Concerning the characterization of packaging steel for finite element analysis, Knieps et al. pointed out different characterization approaches to enable a suitable strategy for packaging steel [4,5]. However, the investigations only focused on sheet metal behavior and not on mechanical properties in the can wall. To enable a prediction of the mechanical properties in the call wall, either the whole process including the ironing must be simulated, or the mechanical properties must be measured directly from the can wall. FE-simulations of the ironing process were shown in general by Dankert et al. [6] and in detail for tinplate products by Nam and Han [7]. However, the simulation of the ironing process leads to high computational cost and is not able to consider the aging behavior afterwards which results from lacquering. Thus, aim of this work is to enable a precise simulation of axial load resistance and paneling pressure for D&I food cans. The results will be used to point out the downgauging potential by using D&I Solid material with an optimized bead geometry.

## 2 Materials and Characterization

To simulate the structural behavior of D&I food cans, four different materials were investigated as they are stated in Table 1. Temper specifications are standardized in DIN EN10202:2022 [8]. All are ferritic steels with a low carbon content in a thickness of 0.28 mm or 0.25 mm and were produced at thyssenkrupp Rasselstein in Andernach. They mainly differ in several production parameters, which results in a higher strength and hardening behavior of the D&I Solid material. This material enables a higher axial load behavior, due to its higher strength.

| | Temper | Thickness, mm | Strength, MPa |
|---|---|---|---|
| D&I Std | TH330 | 0.28 | 305 |
| D&I Solid | - | 0.28 | 384 |
| D&I Std | TH330 | 0.25 | 334 |
| D&I Solid | - | 0.25 | 394 |

*Table 1: Steel specification*

The lower thickness results in a slightly higher strength behavior due to higher rolling degrees and the resulting hardening. However, the strength behavior after the ironing process in the can wall is from utmost importance. Therefore, tensile tests from the can wall were conducted with a measuring length of 50 mm. Specimens were taken in transversal direction from the can wall and afterwards milled to the final geometry. To receive precise strain results, tests were done using an optical measurement system ARAMIS. Since the final strength is not only a function of initial strength but also of the ironing degree, for material D&I Std and D&I Solid tensile test from the can wall were conducted with two different can wall thicknesses (0.12 mm and 0.10 mm). To evaluate the transition between elastic and plastic deformation, it is crucial to adjust the area of elastic deformation correctly, when transforming the stress-strain curve towards a flow curve. In Fig 1b six different flow curves of the different material, sheet thickness and can wall thickness (ironing degree) combinations are shown. It can be clearly seen that the usage of the higher strength D&I solid material leads to a higher strength in the can wall. As well, this figure shows the higher hardening potential of the D&I Solid steel when considering the two different ironing degrees.
When reducing sheet thickness without adapting can manufacturing parameters like blank diameter (cut edge) and trimming, the can wall thickness is a linear function of the initial sheet thickness as it can be observed in Fig 1a.

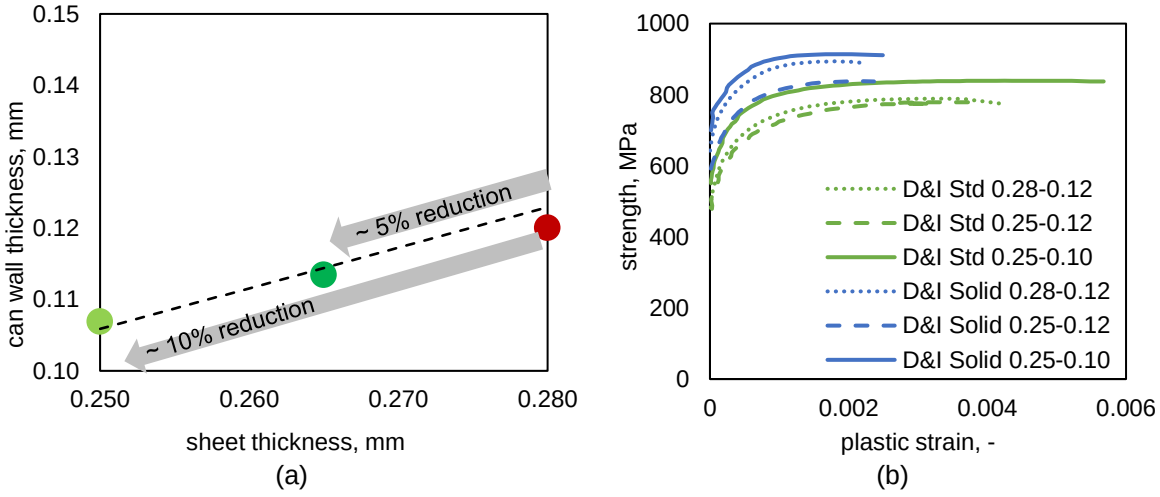


*Fig 1 (a) Can wall thickness as a function of sheet thickness to keep same cutting diameter (b) strength in the can wall measured by tensile tests*

Thus, sheet thickness reduction of 5% starting from a sheet thickness of 0.28 mm and can wall thickness of 0.12 mm results in a can wall thickness of 0.113 mm. A corresponding reduction of 10% results in a can wall thickness of 0.107 mm. As there is no possibility to calculate the final strength of a downgauged material when using FEA, the experimentally measured strength points are interpolated by considering the initial strength behavior and the hardening behavior as a function of the logarithmic strain during forming. This enables to approximate the final strength by estimating the sheet strength for a material of 0.265 mm (~5%) and the corresponding hardening behavior. Both interpolations are shown in Fig 2 and enable the strength approximation. As well, the higher strength can be observed but also the

hardening behavior of the D&I Solid material in comparison to the D&I Std material. Resulting equations to calculate the strength behavior of thickness reduced materials in the can wall are stated in eq. 1-3. They result from the summation of the two equations in Fig 2.

$$Stength_{Canwall} = \sigma_{strenth\ sheet\ metal} + \Delta\sigma_{hardening\ during\ ironing} \quad (1)$$

$$Stength_{Canwall\ D\&I\ Solid} = -448 * Sheet\ thickness + 672 * \varphi + 210 \quad (2)$$

$$Stength_{Canwall\ D\&I\ Std} = -992 * Sheet\ thickness + 356 * \varphi + 486 \quad (3)$$

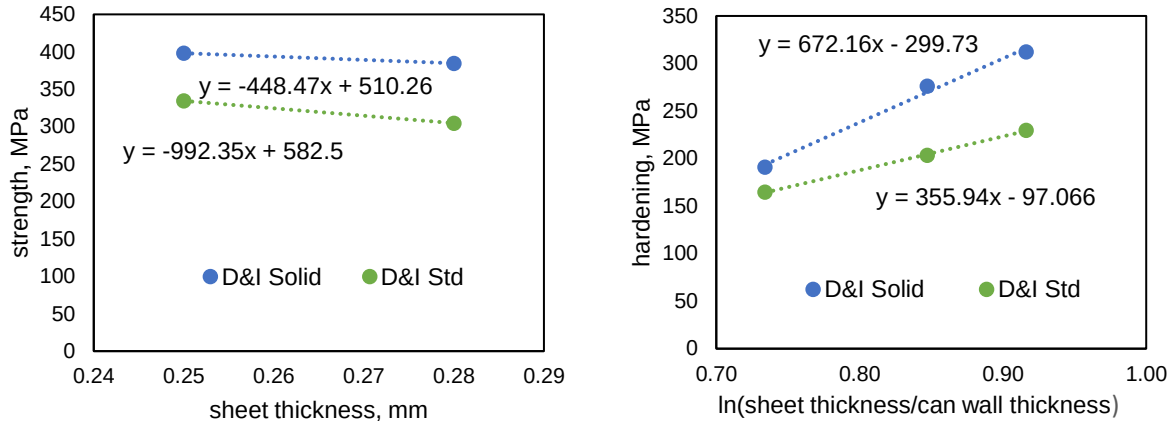


(a) (b)

*Fig 2 Modelling the yield strength in the can wall as a function of initial sheet thickness and ironing degree: (a) yield strength of sheet metal for D&I Std and D&I Solid (b) Hardening of D&I Std and D&I Solid during ironing*

## 3 Model Setup

The complete can model consist of four parts: can body, bottom, lid and seam. All parts of the can are connected using the same nodes, so no contact is required. The can wall has as a mesh size of about 0.3 mm. The mesh size for the other parts is chosen respectively. Also, the material card for the can wall is the same as in axial stability simulations whereas for the bottom the material card of the undeformed material is used and for the lid and seam a material card of a TS550 packaging steel. As the lid and the seam are only relevant for the paneling resistance, the precise modeling of the material behavior is not crucial. The thickness of the seam is calculated as

$$thickness_{seam} = 2 \cdot thickness_{can\ wall} + 3 \cdot thickness_{lid} \quad (4)$$

## 4 Simulation of Axial Stability

To simulate axial resistance of a D&I food can in LS-Dyna, the model was set up as stated in Fig 3. To save computational costs, only the can wall is modelled as bottom and lid have no influence on the axial stability behavior. The element size was chosen as 0.3 mm. This corresponds to about 11 elements over the bead radius when considering a bead width of about 3.57 mm. The mesh size was evaluated in a convergence study. The force to simulate the axial load is applied by a rigid plate, while the bottom is also modelled as rigid plate. In addition, the top node-set is restricted and cannot move in all six degrees of freedom. The bottom node set is just restricted in axial transversal direction. To implement the strength behavior of the material in the can wall a material model `*MAT_PIECEWISE_LINEAR_PLASTICITY` was considered. This material model was only parametrized by the yield strength as calculated in eq. 1-3. Contact is modelled as self-contact for the can and as surface-to-surface contact between can and plate with a friction coefficient of 0.1. To handle the simulation most stable, the motion of the plate is path controlled. Simulations were run implicit using solver mpp d R11.0.0 and a timestep between 0.001 and 0.01 (total time 1 /s and 7.5 mm/s plate travel velocity). To evaluate the axial stability, the force-time curve was exported and the maximum force evaluated. To validate simulation results, they were compared to different experimentally measured values. Those experimentally measured values were evaluated out of axial load experiments, which were conducted at a hydraulic Wolpert press. Fig 3 shows the comparison between experimental and simulated axial load results. The validation was done for three cans differing in material, sheet thickness and resulting wall thickness while having the same bead geometry. The difference between simulated and axial load resistance lies in-between a range of 0.05% deviation and 4.9% deviation (mean 2.2%).

At this point, we can state that the simulation is able to produce comparable axial load resistance values. This gets even more obvious when looking at the standard deviation of experimental values, which lies in a range between 0.035 and 0.05. Crucial for a precise simulation of the axial load resistance is the precise description of the plastic yielding.

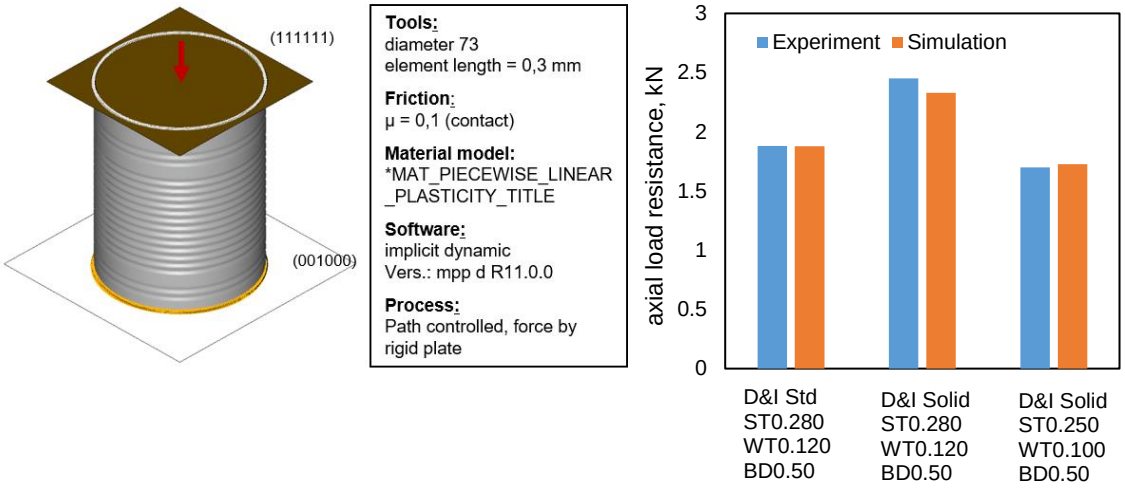


(a) (b)

*Fig 3 Simulation of axial stability: (a) model setup (b) comparison between experiment and simulation*

## 5 Simulation of Paneling Resistance

For the simulation of paneling resistance - the point at which the can implodes due to external pressure - it is assumed that the can implodes in the shape of an eigenmode. In contrast to the calculation of axial stability, bottom, lid and seam must be considered in the calculation of paneling resistance as they have an influence on the eigenmoden Fig 4a. The eigenmoden are calculated in a separate simulation before the stability simulation using the keyword `*CONTROL_IMPLICIT_EIGENVALUE`. To allow the can to deform in a natural shape the can is not fully constrained. For the eigenvalue analysis only three nodes in the middle plane of the can, spanning an equilateral triangle, are constrained in z-direction. Comparison of experiment and eigenvalue simulation shows that the can implodes in the shape of the lowest eigenmode with positive slope Fig 4b.

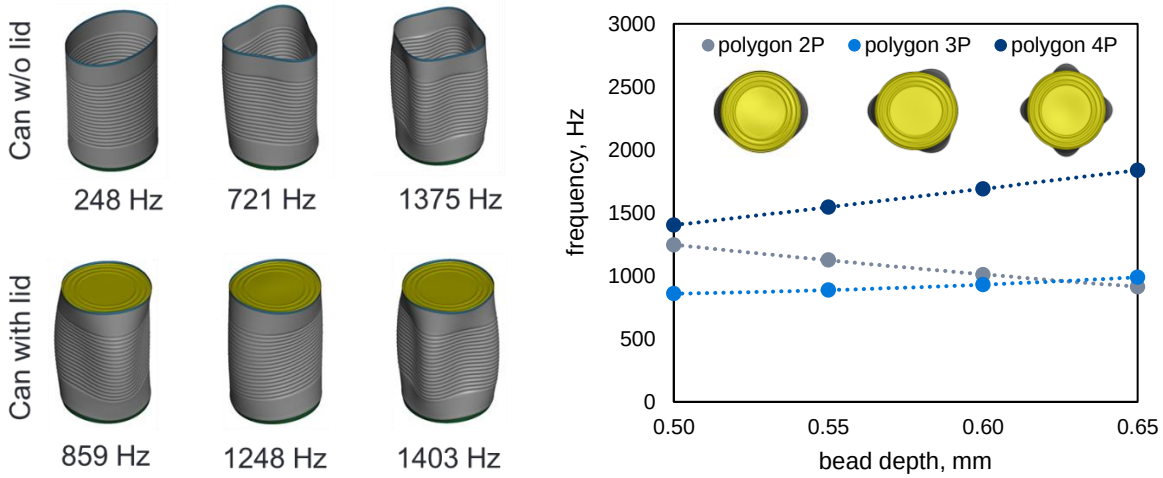


(a) (b)

*Fig 4 Eigenmode analysis of D&I food cans: (a) comparison of Eigen frequency with and without lid (b) development of the Eigen frequency as a function of bead depth*

The nodal displacements of the respective eigenmode are written to a file for each direction and will be used to perturb the can in the stability simulation. As stated in [9] modeling an imperfection is crucial for the stability analysis. The keyword `*PERTURBATION_NODE` is used to read in the files from the eigenvalue analysis and perturb the can with the shape of an eigenmode. For a 73 mm can diameter

and a three-point polygon shape the min/max values of nodal displacement are -6.55 / 3.28 mm in x-direction and +/- 5.67 mm in y-direction. As it can be seen in Fig 5, no realistic results can be achieved without perturbation. On the other hand, a higher perturbation results in a lower stability value. A scale factor (SCL) of 0.001 results in a deviation between simulation and experiment of 0.9% resp. 2.9%, which is within the range of the standard deviation of the experiment. A SCL of 0.01 lowers the calculated stability for this can size about 6.7 +/- 0.1% but avoids outliers. Therefore, a SCL of 0.01 was chosen for the simulations.

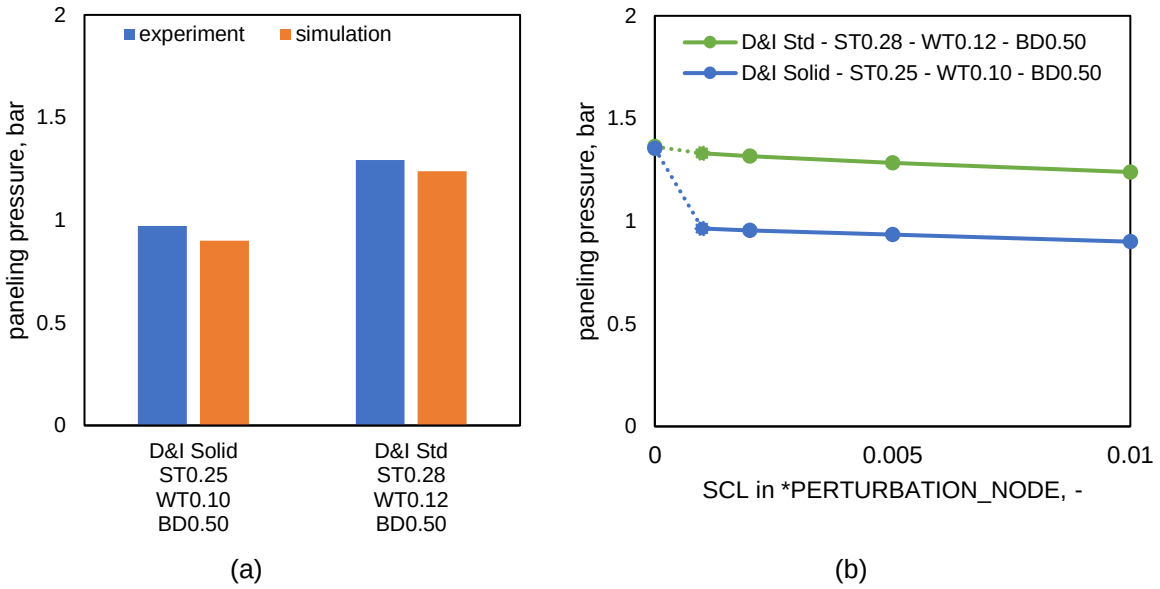


*Fig 5 Simulation of paneling resistance (a) comparison between experiment and simulation (b) influence of perturbation degree on the paneling pressure*

In contrast to the eigenvalue analysis, where only three nodes were constrained, the keyword `*CONTROL_IMPLICIT_INERTIA_RELIEF` is used to suppress the rigid-body motion when simulating the paneling resistance. This is especially important when using arc length method since it requires a termination condition. In this case the option `*TERMINATION_NODE` is used to determine the onset of implosion. Since this method lowers the maximum load (Fig 6a), the termination condition should be close to this point to ensure that the termination condition is met. The load is applied to a shell set consisting of can wall, bottom and lid with a load curve starting at 0 bar at the beginning of the simulation and reaching 3 bar at 1 second. Thus, time and load magnitude are related by a constant. With comparable results, the arc length method allows a significant reduction of computation time by a factor of 2 to 6 (Fig 6b).

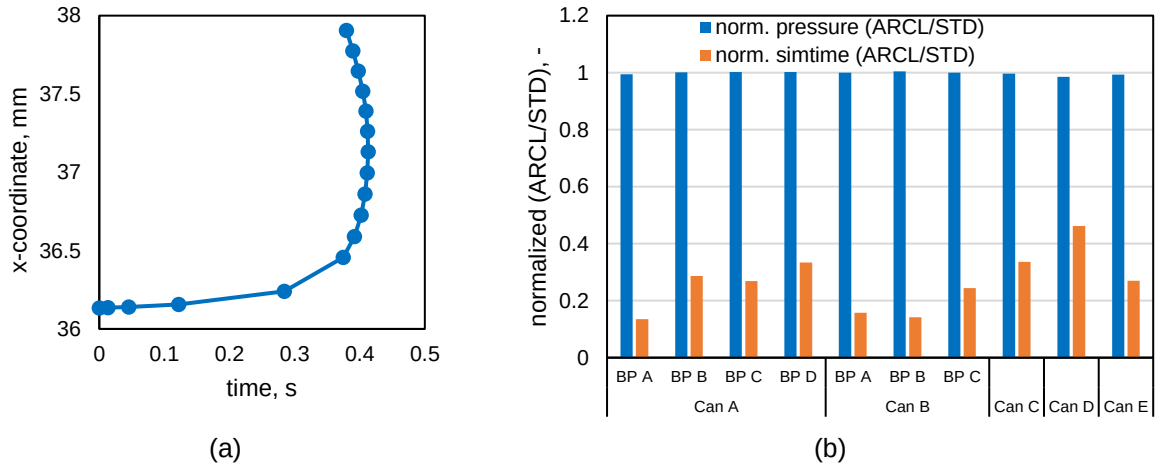


*Fig 6 Optimization of computational costs: (a) `*TERMINATION_NODE` (b) arc-length method*

## 6 Can Optimization

To find a bead depth, which meets the stability of the reference can (wall thickness of 0.120 mm, bead depth of 0.50 mm and D&I Std material) axial load and paneling resistance are simulated for three different material thicknesses and four different bead depths as shown in Table 2.

| Material | Material thickness, mm | Wall thickness, mm | Bead depth, mm | Tool: No-bead distance-radius |
|---|---|---|---|---|
| D&I Std. | 0.280 | 0.120 | 0.50 | W3-3.56-R0.75 |
| D&I Solid | 0.280 | 0.120 | 0.50 | W3-3.56-R0.75 |
| D&I Solid | 0.280 | 0.120 | 0.55 | W3-3.56-R0.75 |
| D&I Solid | 0.280 | 0.120 | 0.60 | W3-3.56-R0.75 |
| D&I Solid | 0.280 | 0.120 | 0.65 | W3-3.56-R0.75 |
| D&I Solid | 0.265 | 0.113 | 0.50 | W3-3.56-R0.75 |
| D&I Solid | 0.265 | 0.113 | 0.55 | W3-3.56-R0.75 |
| D&I Solid | 0.265 | 0.113 | 0.60 | W3-3.56-R0.75 |
| D&I Solid | 0.265 | 0.113 | 0.65 | W3-3.56-R0.75 |
| D&I Solid | 0.250 | 0.107 | 0.50 | W3-3.56-R0.75 |
| D&I Solid | 0.250 | 0.107 | 0.55 | W3-3.56-R0.75 |
| D&I Solid | 0.250 | 0.107 | 0.60 | W3-3.56-R0.75 |
| D&I Solid | 0.250 | 0.107 | 0.65 | W3-3.56-R0.75 |

*Table 2 Different combination of initial thickness and bead geometry for simulation of axial load and paneling resistance*

Those twelve combinations use D&I Solid material as this is one of the next-generation high-strength D&I steel grades whereas the tool is the same as for the reference can with standard D&I material. The goal is to find a combination that meets the stability values of the reference can, which was made from D&I Std material. The results for axial load resistance and paneling resistance are shown in Fig 7. As expected, axial load resistance decreases with lower wall thickness and higher bead depth. There is a linear relation between axial load and bead depth. Using D&I Solid material without change of wall thickness results in an increase of around 20% in axial stability at the same bead depth. The bead depth can be increased up to 0.65 mm without falling below the stability limit. For a wall thickness of 0.113 mm axial load is better or comparable up to a bead depth of 0.57 mm. For a wall thickness of 0.107 mm the stability of the standard can is met only at a bead depth of 0.5 mm.
Paneling resistance shows a stability decrease with lower wall thickness but an increase with higher bead depth. The relation between paneling resistance and bead depth is quadratic. Since the yield strength in can wall has only a very minor influence on the paneling resistance, there are no advantages for the wall thickness 0.120 mm compared to the reference can. However, since an increased bead depth leads to higher paneling resistance, all variants with a wall thickness of 0.120 mm are above the required value. For a wall thickness of 0.113 mm, a bead depth of 0.55 mm and more meets the required value; for a wall thickness of 0.107 mm, this is the case from a bead depth of 0.59 mm.

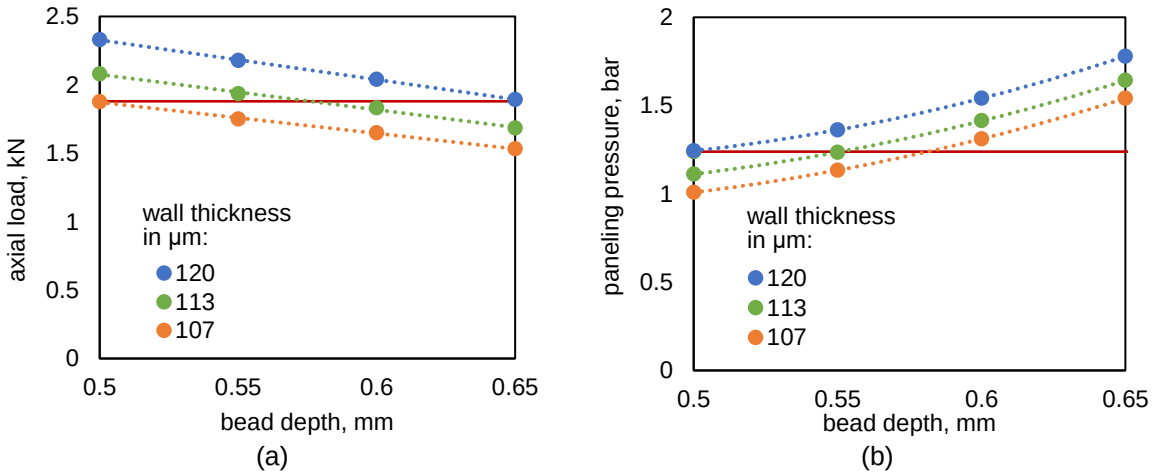


*Fig 7 Simulation results: effect of wall thickness and bead depth on (a) axial load (b) paneling resistance*

Simulating several combinations of bead depth and thickness, the use of D&I Solid revealed a downgauging potential of about 5%. This can be done by reducing the can wall to 0.113 mm and increasing the bead depth up to 0.55 mm to hold the paneling resistance. Further reduction potential requires the development of a next generation D&I Solid steel with an even higher yield strength and thus a higher axial load potential.

## 7 Summary

Based on the main findings, the following conclusions can be drawn:

- To simulate axial stability of D&I food cans, it is essential to model the strength in the can wall precisely. Therefore, in this work, tensile tests out of ironed cans were conducted. Simulating axial stability based on the strength in the can wall revealed good results in comparison to experimental stability values.
- To simulate paneling resistance of D&I food cans, it is mandatory to consider the eigenmoden by an eigenvalue analysis. By this, perturbation was done by the lowest eigenmode with a positive slope, which revealed very good results when simulating paneling resistance in comparison to experimental values.
- By using both, simulation of axial stability and paneling resistance, the downgauging potential of D&I food cans of about 5% could be shown when using higher strength D&I Solid material. This revealed the great potential to optimize can weight and CO2 footprint by using FE-simulation while reducing cost intensive trial and error experiments.

The results also showed further downgauging potential of up to 10% when using steels with an even higher yield strength. At the same time, these kinds of steels are not developed yet for D&I applications. As well the IGA method [10] offers great potential to model the can wall without the fine discretization in the bead radius. Precision and computational costs might be optimized by using this approach.

## 8 Literature

[1] M. Köhl, F. Knieps, I. Weinand, B. Liebscher, Effiziente Produktentwicklung in der Verpackungsstahlindustrie durch Nutzen von FE-Methoden, in: 33. Aachen Stahlkolloquium 2022.
[2] Linear and Nonlinear Buckling Analysis and Flange Crippling, Engineering Mechanics White Paper 2012.
[3] J. Wang, Design optimization of rigid metal containers, Finite Elements in Analysis and Design 37 (2001) 273–286. https://doi.org/10.1016/S0168-874X(00)00043-3.
[4] F. Knieps, M. Köhl, M. Merklein, Local Strain Measurement in Tensile Test for an Optimized Characterization of Packaging Steel for Finite Element Analysis, KEM 883 (2021) 309–316. https://doi.org/10.4028/www.scientific.net/KEM.883.309.
[5] F. Knieps, B. Liebscher, I. Moldovan, M. Köhl, J. Lohmar, Characterization of High-Strength Packaging Steels: Obtaining Material Data for Precise Finite Element Process Modelling, Metals 10 (2020) 1683. https://doi.org/10.3390/met10121683.
[6] J. Danckert, The Residual Stress Distribution in the Wall of a Deep-Drawn and Ironed Cup Determined Experimentally and by FEM, CIRP Annals 43 (1994) 249–252. https://doi.org/10.1016/S0007-8506(07)62206-9.
[7] Jaebok Nam, Kyung Seop Han, Finite Element Analysis of Deep Drawing and Ironing Process in the Steel D & I, in: Materials Science.
[8] DIN, Kaltgewalzte Verpackungsblecherzeugnisse – Elektrolytisch verzinnter und spezialverchromter Stahl Deutsche Fassung EN 10202:2001, Beuth Verlag GmbH, 2001.
[9] Creating imperfections in LS-DYNA® using the *PERTURBATION keyword, 2023, https://www.lsoptsupport.com/howtos/creating-imperfections-in-ls-dyna-r-using-the-perturbation-keyword.
[10] T. Hughes, J.A. Cottrell, Y. Bazilevs, Isogeometric analysis: CAD, finite elements, NURBS, exact geometry and mesh refinement, Computer Methods in Applied Mechanics and Engineering 194 (2005) 4135–4195. https://doi.org/10.1016/j.cma.2004.10.008.